



Received: 24 September 2017
Accepted: 27 November 2017
First Published: 05 December 2017

*Corresponding author: Department of Physics, University of Alabama at Birmingham, Birmingham, AL 35294, USA
E-mail: ykvohra@uab.edu

Reviewing editor:
Ahuja Rajeev, Uppsala University, Sweden

Additional information is available at the end of the article

CONDENSED MATTER PHYSICS | RESEARCH ARTICLE

Near-zero thermal expansion in magnetically ordered state in dysprosium at high pressures and low temperatures

Kevin M. Hope¹, Gopi K. Samudrala² and Yogesh K. Vohra^{2*}

Abstract: The atomic volume of rare earth metal dysprosium (Dy) has been measured up to high pressures of 35 GPa and low temperatures between 200 and 7 K in a diamond anvil cell using angle dispersive X-ray diffraction at a synchrotron source. The hexagonal close-packed (*hcp*), alpha-Samarium (α -*Sm*), and double hexagonal close-packed (*dhcp*) phases are observed to be stable in Dy under high-pressure and low-temperature conditions achieved in our experiments. Dy is known to undergo magnetic ordering below 176 K at ambient pressure with magnetic ordering Néel temperature (T_N) that changes rapidly with increasing pressure. Our experimental measurement shows that Dy has near-zero thermal expansion in the magnetically ordered state and normal thermal expansion in the paramagnetic state for all the three known high pressure phases (*hcp*, α -*Sm*, and *dhcp*) to 35 GPa. This near-zero thermal expansion behavior in Dy is observed below the magnetic ordering temperature T_N at all pressures up to 35 GPa.

ABOUT THE AUTHORS

The high-pressure structural and magnetic phase transition study on rare earth metal dysprosium at high pressures and low temperatures is carried out by Yogesh Vohra's research group at the University of Alabama at Birmingham (UAB) and is supported by the US Department of Energy – National Nuclear Security Administration. This is part of a larger study on structural, electronic, and magnetic transitions in transition metals, rare earth metals and their alloys under extreme conditions of pressure and temperatures. Yogesh Vohra is the founding director of UAB Center for Nanoscale Materials and Biointegration (CNMB) that houses a Diamond Microfabrication Laboratory. Yogesh Vohra's research group has also pioneered several enabling technologies used in studies of materials under extreme conditions including diamond anvils with embedded sensors (designer diamonds) and nanocrystalline diamond micro-anvils grown by chemical vapor deposition techniques to study materials to pressures exceeding 500 GPa.

PUBLIC INTEREST STATEMENT

Rare earth elements are extensively utilized in a variety of applications including strong permanent magnets, lasers, lighting industry, automobiles, nuclear industry, and medicine. With one of the highest intrinsic magnetic moments (10.6 Bohr Magnetron) among the heavy rare earth elements, dysprosium (Dy) exhibits a rich magnetic phase diagram under high-pressure and low-temperature conditions. On cooling below 176 K, Dy shows spatial ordering of its magnetic moments on ions at the crystalline sites that are accompanied by unusual thermal expansion properties. Our paper reports on the relationship between magnetic ordering and near-zero thermal expansion observed in Dy at low temperatures. Furthermore, our X-ray diffraction measurements combined with magnetic ordering studies at high pressures and low temperatures reveal that the correlation between magnetic ordering and near-zero thermal expansion is observed in all known high pressure phases of Dy to 35 GPa. The connection between lack of thermal expansion and magnetic ordering is likely a universal phenomenon for rare earth metals under extreme conditions.

Subjects: Material Science; Materials Science; Physics

Keywords: magnetic ordering; rare earth metals; high pressures; low temperatures; thermal expansion

PACS codes: 62.50.-p; 75.30.Kz; 75.25.-j; 61.05.F-

1. Introduction

With one of the highest intrinsic magnetic moments (10.6 Bohr Magnetron) among the heavy rare earth elements, dysprosium (Dy) exhibits a rich magnetic phase diagram under high-pressure and low-temperature conditions. The structural phase transitions in 4f-lanthanide metals have been recently reviewed to ultra-high pressures up to 200 GPa and the crystal structure trends with increasing pressure have been well documented (Samudrala & Vohra, 2013). The crystallographic sequence $hcp \rightarrow \alpha\text{-Sm} \rightarrow dhcp \rightarrow fcc - \text{distorted } fcc$ is observed with increasing pressure or decreasing atomic number in all lanthanide metals and is explained on the basis of number of *d*-electrons facilitated by electron transfer from the *s*-conduction band to the *d*-conduction band under high pressures (Duthie & Pettifor, 1977; Johansson & Rosengren, 1975). At the same time, lanthanide metal ions contain an un-filled *f*-shell and localized magnetic moments that show magnetic ordering at low temperatures due to interplay between strong correlation effects and indirect exchange effects involving their *f*-electrons. The magnetic ordering transitions in heavy lanthanides have been studied by magnetic susceptibility measurements in a diamond anvil cell up to modest pressure of 10–20 GPa and a systematic decrease in magnetic ordering temperature with increasing pressure has been documented (Jackson, Malba, Weir, Baker, & Vohra, 2005). The recent innovations in measurements of magnetic ordering temperature in rare earth metals by electrical transport techniques have revealed complex magnetic behavior in Dy and have extended magnetic measurements to megabar pressures (Lim, Fabbris, Haskel, & Schilling, 2015; Samudrala, Tsoi, Weir, & Vohra, 2014). It has been shown previously (Samudrala et al., 2014) that the electrical transport measurement is a very sensitive technique for measuring magnetic ordering temperatures in rare earth metals and these measurements have been validated by direct observation of magnetic structures by neutron diffraction studies at high pressures and low temperatures (Thomas, Tsoi, Wenger, & Vohra, 2011; Thomas et al., 2013). The magnetic ordering temperature information coupled with atomic volume measurements by X-ray diffraction at high pressures and low temperatures allows for direct correlation between the thermal expansion and the magnetic ordering in 4-f metals under compression.

At ambient pressure, the paramagnetic (PM) to anti-ferromagnetic (AFM) transition at $T_N = 176$ K and AFM to ferromagnetic (FM) transition at $T_C = 87$ K are well documented in Dy (Legvold, Spedding, Barson, & Elliott, 1953). A helical magnetic structure is observed between 87 and 176 K at ambient pressure whereby the magnetization is always in the basal plane perpendicular to the *c*-axis but changes in direction from one hexagonal close-packed plane to the next with a turn angle that is temperature and pressure dependent. This turn angle has been measured at ambient pressure by neutron diffraction studies and increases almost linearly with temperature from 27° at 87 K to 43° per layer at 176 K (Wilkinson, Koehler, Wollan, & Cable, 1961). The magnetic ordering transition temperature in Dy shows a decrease with increasing pressure in the *hcp*-phase followed by a discontinuous drop in transition to the $\alpha\text{-Sm}$ phase (Samudrala et al., 2014). The magnetic ordering transition then undergoes through a minimum and then increases with further increase in pressure in the *dhcp*-phase to 35 GPa (Samudrala et al., 2014). Dy also shows unconventional magnetic state under ultra-high pressures as the magnetic ordering temperature increases rapidly above 73 GPa (above pressure of volume collapse) and attains a value greater than ambient temperature of 300 K at pressures above 107 GPa (Lim et al., 2015).

The anomalous thermal expansion and magnetostriction in single-crystal Dy at ambient pressure are well established (Clark, DeSavage, & Bozorth, 1965). In the paramagnetic phase, the thermal expansion is normal and as the temperature is lowered and the spins align and terms in thermal expansion attributed to thermal vibrations are dwarfed by those arising from the magneto elastic energy (Clark et al., 1965). As a result, *c*-axis expands on cooling below the anti-ferromagnetic phase, while *a*-axis shows normal contraction with decreasing temperature as revealed by direct X-ray diffraction studies at low temperatures and ambient pressure (Darnell & Moore, 1963). This gives rise to anomalous thermal expansion in Dy below the Néel temperature T_N and discontinuous changes in *c*-axis expansion and *a*-axis contraction on further cooling to ferromagnetic phase below 87 K (Darnell & Moore, 1963). Our experimental study is motivated by studying the effect of high pressure on this anomalous thermal expansion behavior in Dy. In particular, we are investigating the role of phase transitions to various close-packed structures under compression in Dy and their effect in anomalous thermal expansion behavior. Our experiments provide for a direct correlation between the structural data and the magnetic transition temperature measurements in Dy under simultaneous high-pressure low-temperature conditions.

2. Experimental details

X-ray diffraction experiments on polycrystalline Dy were carried out at the beam-line 16-BM-D, HPCAT, Advanced Photon Source at Argonne National Laboratory to low temperatures of 7 K using a diamond anvil cell. The Dy sample of 99.99% purity was placed in a sample chamber of 80 micron in diameter and 40 micron in thickness in a spring steel gasket along with a ruby pressure sensor in a diamond anvil cell. An angle-dispersive technique with an image-plate area detector was employed using an X-ray wavelength $\lambda = 0.4246 \text{ \AA}$. For simultaneous temperature- and pressure-dependent X-ray diffraction experiments, the diamond anvil cell (DAC) was cooled in a continuous helium flow-type cryostat, and the pressure in the cell was measured *in situ* with the ruby fluorescence technique (Tsoi et al., 2009; Yen & Nicol, 1992). The image plate XRD patterns were recorded with a focused X-ray beam of $6 \mu\text{m}$ by $13 \mu\text{m}$ (FWHM) on sample mixed with ruby, which served as the pressure marker. The Dy sample-to-image plate detector distance was calibrated using CeO_2 diffraction pattern and was measured to be 341.12 mm and was held constant throughout the entirety of the experiment. The software package FIT2D (Hammersley, 1995) was used to integrate the collected MAR345 image plate diffraction patterns which were analyzed by GSAS (Larson & Von Dreele, 2004) software package with EXPGUI interface (Toby, 2001) employing full-pattern Rietveld refinements to extract lattice parameters.

3. Results and discussion

The methodology we have utilized for determining Néel temperature (T_N) from electrical transport measurements and the effectiveness of this technique have been described in detail elsewhere (Lim et al., 2015; Samudrala et al., 2014; Thomas et al., 2011, 2013). Figure 1 shows four-probe electrical resistance data for Dy as a function of temperature at pressures of 1.1 GPa. The magnetic transition temperature has been determined by finding out the lowest point in the temperature derivative of resistance data (dR/dT) as shown in Figure 1. It can be readily seen that the derivative of the resistance has a clear minimum and this has been taken as the Néel temperature (T_N). The experimentally determined value of 175 K agrees very well with the ambient pressure T_N value of dysprosium, which is 179 K.

Figure 2 shows the magnetic ordering temperature as a function of pressure in various phases of Dy to 35 GPa. Dy shows an initial decrease in Néel temperature (T_N) with pressure at a rate of -5.7 Kelvin/GPa in agreement with previously published data (Jackson et al., 2005). The structural phase transition $hcp \rightarrow Sm$ occurs at 7 GPa, and $Sm \rightarrow dhcp$ transition occurs at 17 GPa as illustrated in the magnetic phase diagram in Figure 1. There is an abrupt drop in T_N on transition to *Sm*-phase at 7 GPa followed by a gradual decrease till 17 GPa before transition to *dhcp*-phase. T_N increases with

Figure 1. The four-probe electrical resistance measurement on the *hcp* phase of Dy as a function of temperature at a pressure of 1.1 GPa (left vertical axis).

Note: The anti-ferromagnetic transition temperature (T_N) is marked by a resistance anomaly that is best represented by a minimum in the derivative of resistance with temperature (dR/dT) curve also shown (right vertical scale).

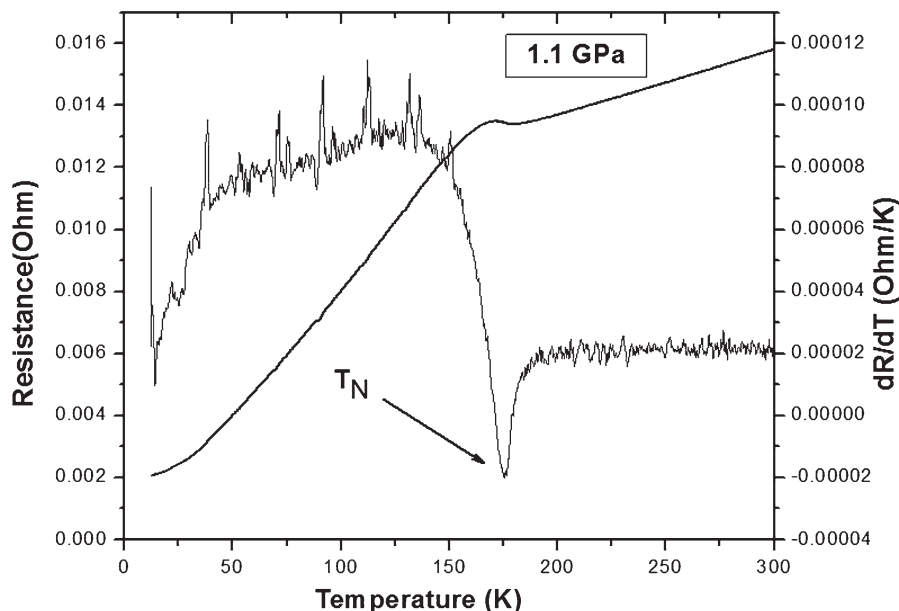
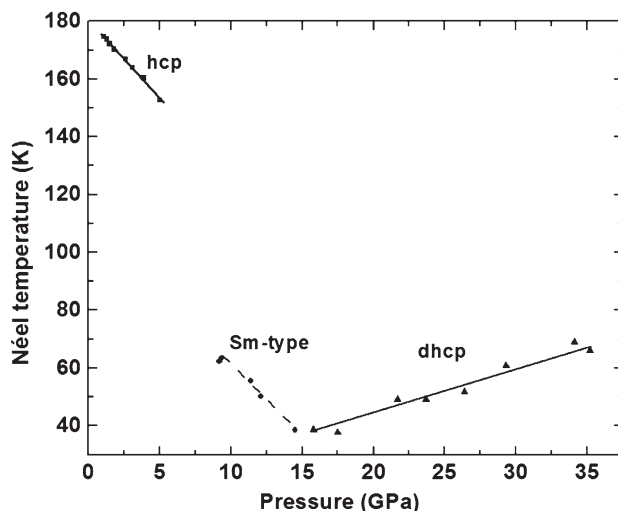


Figure 2. Magnetic ordering Néel temperature for Dy as a function of pressure up to 35 GPa with data adapted from Samudrala et al. (2014).

Note: The solid lines are the linear fit to the data as described in the text. The three known crystal structures *hcp*, *Sm-type*, and *dhcp* at high pressures and low temperatures for Dy are indicated in the graph.



increasing pressure in the *dhcp*-phase. The magnetic ordering Néel temperature (T_N) for Dy has been fitted as a linear function of pressure in Figure 2 for various phases as shown below for pressures up to 35 GPa.

$$T_N = -5.7221P + 181.28 \text{ (hcp - phase)}$$

$$T_N = -4.6002P + 105.96 \text{ (}\alpha\text{-Sm - phase)}$$

$$T_N = 1.6094P + 11.834 \text{ (dhcp - phase)}$$

Figure 3 shows the image plate angle-dispersive X-ray diffraction patterns at high pressures up to 35 GPa and temperatures down to 7 K for *hcp*, α -Sm, and *dhcp*-phases for Dy. Figure 4 shows the integrated X-ray diffraction patterns for the *hcp*, α -Sm, and *dhcp*-phase of Dy that were analyzed using Rietveld refinement to obtain atomic volume at high pressures and low temperatures. The measured lattice parameters and refinement parameters at high pressures and low temperatures

Figure 3. Image plate angle-dispersive X-ray diffraction data for Dy at high pressures and low temperatures utilized in the measurements of thermal expansion. The X-ray wavelength $\lambda = 0.4246 \text{ \AA}$ and Dy sample-to-image plate distance is 341.12 mm (a) Temperature 7 K and pressure 1.7GPa in the *hcp* phase, (b) temperature 7 K and pressure 8.6 GPa in the *Sm-type* phase, and (c) temperature 6.8 K and pressure 35.2 GPa in the *dhcp* phase.

Note: The fitted crystal structure data are shown in Table 1.

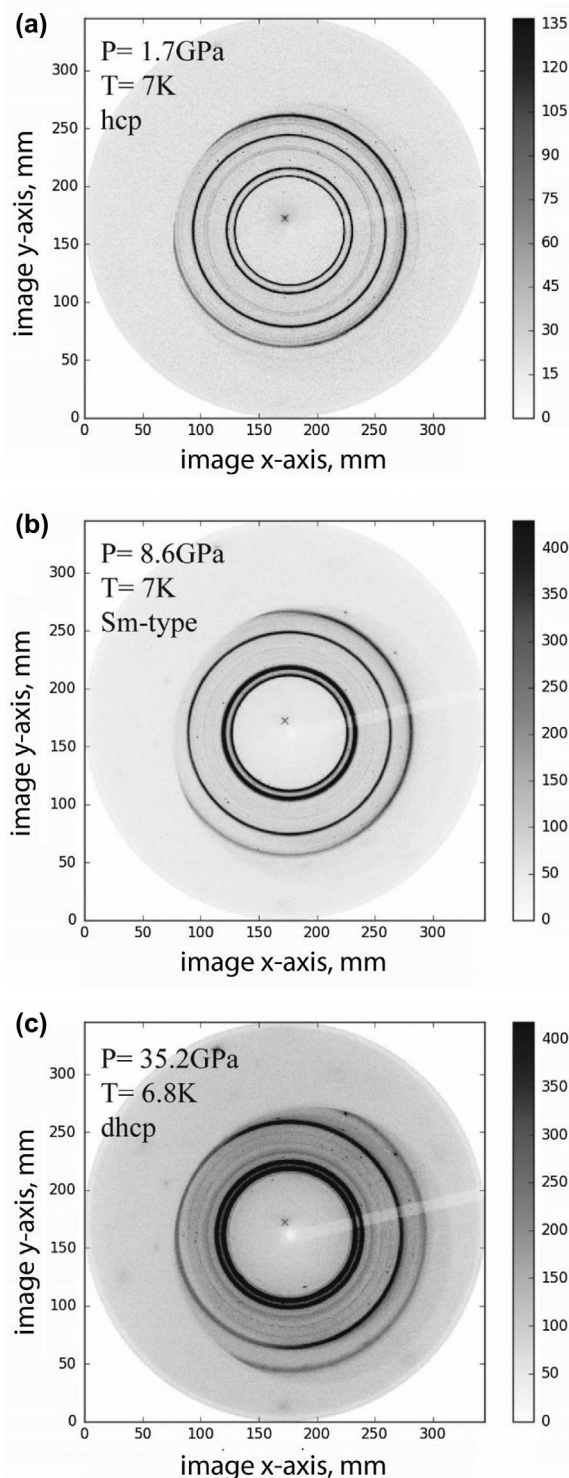


Figure 4. Integrated X-ray diffraction patterns at high pressures and low temperatures for (a) *hcp*, (b) *Sm-type*, and (c) *dhcp* phases of Dy. The diffraction peaks are labeled with the corresponding Miller indices (*hkl*) and the measured lattice parameters are described in Table 1.

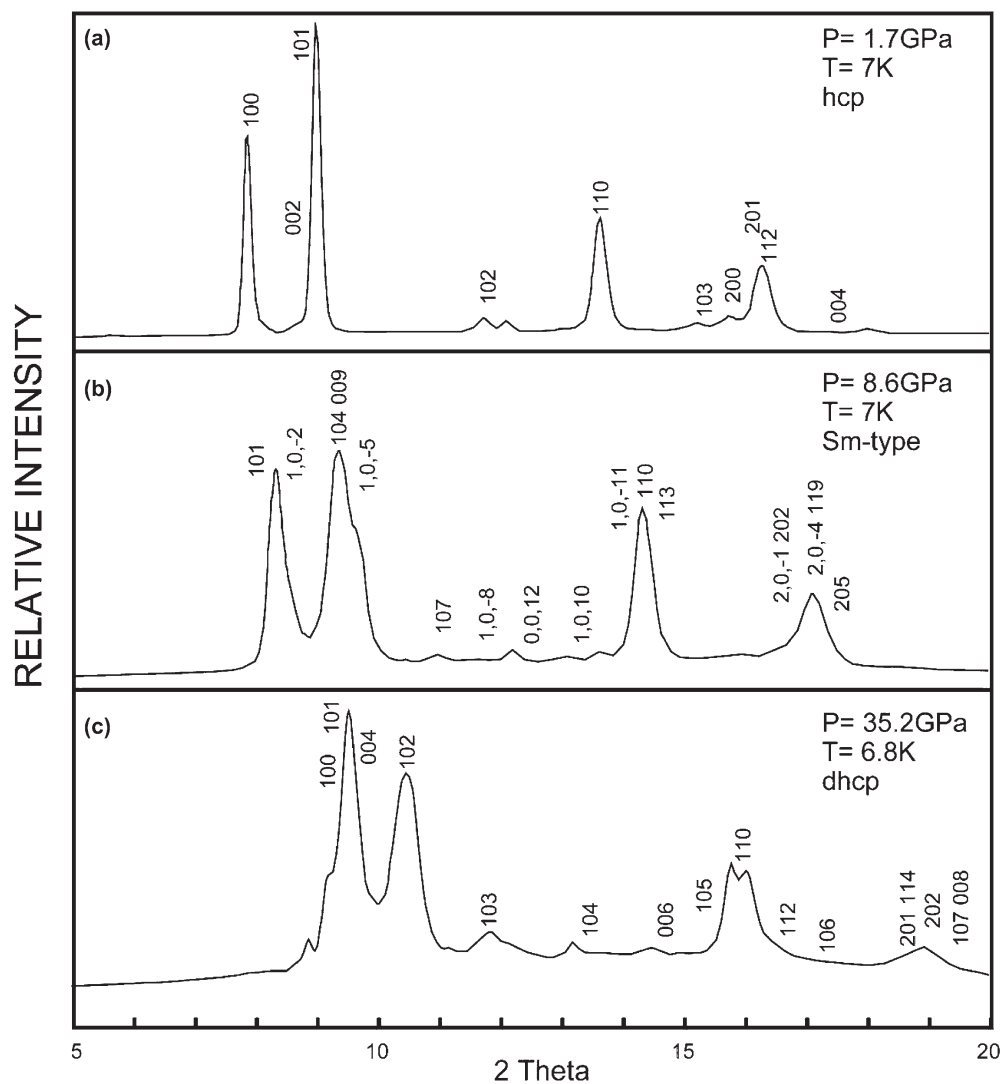


Table 1. The fitted lattice parameters for dysprosium at high pressures and low temperatures

Crystal Structure	Experimental conditions (P, T)	Lattice parameters	Refinement parameter (reduced χ^2)
hcp	1.7 GPa, 7 K	$a = 3.587, c = 5.601$	0.658
		$c/a = 1.562$	
Sm-type	8.6 GPa, 7 K	$a = 3.415, c = 23.574$	2.626
		$c/a = 6.903$	
dhcp	35.2 GPa, 6.8 K	$a = 3.100, c = 10.103$	0.825
		$c/a = 3.259$	

for the three phases of Dy are shown in Table 1. The X-ray diffraction data collected at various pressures and low temperatures between 7 K and 200 K were collated to produce atomic volume maps for Dy.

Figure 5. The normalized change in volume ($\Delta V/V_0$) where V_0 is the measured volume at the lowest temperature plotted as a function of temperature (T) at various pressures. The dashed lines represent the Néel temperature (T_N) at various pressures obtained from data in Figure 1. (a) Dy at 1.5 GPa in the *hcp* phase with $V_0 = 31.20 \text{ \AA}^3/\text{atom}$ at 7 K, (b) Dy at 8.2 GPa in the α -*Sm* phase with $V_0 = 26.44 \text{ \AA}^3/\text{atom}$ at 7 K, (c) dysprosium at 17.2 GPa in the *dhcp* phase with $V_0 = 21.89 \text{ \AA}^3/\text{atom}$ at 9 K, and (d) dysprosium at the highest pressure of 33.9 GPa in the *dhcp* phase with $V_0 = 21.03 \text{ \AA}^3/\text{atom}$ at 9 K.

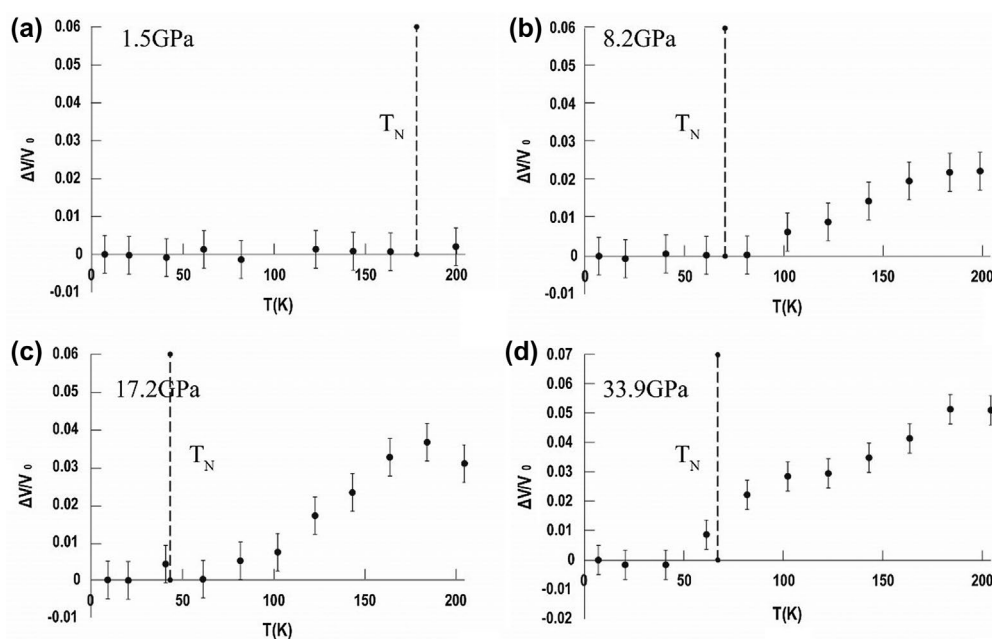


Figure 5 shows the normalized change in atomic volume ($\Delta V/V_0$) as a function of temperature (T) for various pressures as indicated. The ΔV is the change in volume relative to measured volume V_0 at the lowest temperature (generally at 7 K). The data in Figure 5 cover four different pressures of 1.5 GPa ($T_N = 173$ K), 8.2 GPa ($T_N = 68$ K), 17.2 GPa ($T_N = 40$ K), and 33.9 GPa ($T_N = 66$ K). The experimentally measured magnetic ordering temperature (T_N) obtained from fits described earlier (Figure 2) at these pressure is shown as dashed lines in Figure 5. The experimental data at 1.5 GPa for the *hcp* phase show near-zero thermal expansion almost in the entire temperature range with some increase above 173 K. It is clear from Figure 5 that the change in atomic volume with temperature is near-zero for temperature below T_N and rises gradually above the magnetic ordering temperature in the paramagnetic phase. This phenomenon appears to be universal for all high-pressure phases including *hcp*, α -*Sm*, and *dhcp*-phase of Dy to 35 GPa. It should be added that the details of the magnetic ordering in *Sm*-phase and *dhcp*-phase of Dy have not yet been established by neutron diffraction at high pressures and low temperatures. However, the phenomenon of near-zero thermal expansion in Dy appears to be broadly connected with magnetic ordering and is independent of the details of the magnetic structures at high pressures and low temperatures.

In summary, we have shown that the rare earth metal dysprosium exhibits near-zero thermal expansion with temperature in the magnetically ordered phase below Néel temperature (T_N). This correlation is obtained by combining electrical resistance data and X-ray diffraction data obtained at high pressures and low temperatures. This anomalous thermal expansion phenomenon is universal and is observed for all high-pressure phases including *hcp*, α -*Sm*, and *dhcp* to 35 GPa. The anomalous thermal expansion behavior tracks the magnetic transition temperature in dysprosium at high pressures. It is now possible to correlate thermal expansion data at high pressure and low temperature for rare earth metals to the magnetic ordering temperatures determined by electrical transport measurements.

Acknowledgments

We acknowledge assistance from Mr. Chloe Hope in preparation of figures in this manuscript. Portions of this work were performed at HPCAT (Sector 16), Advanced Photon Source (APS), Argonne National Laboratory.

Funding

This work was supported by the Department of Energy-National Nuclear Security Administration [award number

DE-NA0002928]; HPCAT operations are supported by DOE-NNSA [award number DE-NA0001974], [award number DOE-BES] [award number DE-FG02-99ER45775] with partial instrumentation funding by NSF; APS is supported by DOE-BES [contract number DE-AC02-06CH11357].

Author details

Kevin M. Hope¹
E-mail: HopeKM@montevallo.edu

Gopi K. Samudrala²

E-mail: gopi@uab.edu

Yogesh K. Vohra²

E-mail: ykvohra@uab.edu

¹ Department of Biology, Chemistry and Mathematics,
University of Montevallo, Montevallo, AL 35115, USA.

² Department of Physics, University of Alabama at
Birmingham, Birmingham, AL 35294, USA.

Citation information

Cite this article as: Near-zero thermal expansion in magnetically ordered state in dysprosium at high pressures and low temperatures, Kevin M. Hope, Gopi K. Samudrala & Yogesh K. Vohra, *Cogent Physics* (2017), 4: 1412107.

References

- Clark, A. E., DeSavage, B. F., & Bozorth, R. (1965). Anomalous thermal expansion and magnetostriction of single-crystal Dysprosium. *Physical Review*, 138, A216–A224.
- Darnell, F. J., & Moore, E. P. (1963). Crystal structure of dysprosium at low temperatures. *Journal of Applied Physics*, 34, 1337–1338.
<https://doi.org/10.1063/1.1729497>
- Duthie, J. C., & Pettifor, D. G. (1977). Correlation between d-band occupancy and crystal structure in the rare earths. *Physical Review Letters*, 38, 564–567.
<https://doi.org/10.1103/PhysRevLett.38.564>
- Hammersley, A. P. (1995). ESRF internal report (EXP/AH/95-01, FIT2D V5.18 Reference Manual V1.6).
- Jackson, D. D., Malba, V., Weir, S. T., Baker, P. A., & Vohra, Y. K. (2005). High-pressure magnetic susceptibility experiments on the heavy lanthanides Gd, Tb, Dy, Ho, Er, and Tm. *Physical Review*, B71, 184416 1–7.
- Johansson, B., & Rosengren, A. (1975). Generalized phase diagram for the rare-earth elements: Calculations and correlations of bulk properties. *Physical Review*, B11, 2836–2857.
- Larson, A. C., & Von Dreele, R. B. (2004). *General structure analysis system (GSAS)* (Los Alamos National Laboratory Report LAUR, 86-748).
- Legvold, S., Spedding, F. H., Barson, F., & Elliott, J. F. (1953). Some magnetic and electrical properties of gadolinium, dysprosium, and erbium metals. *Reviews of Modern Physics*, 25, 129–130.
<https://doi.org/10.1103/RevModPhys.25.129>
- Lim, J., Fabbri, G., Haskel, D., & Schilling, J. S. (2015). Magnetic ordering at anomalously high temperatures in Dy at extreme pressures. *Physical Review*, B91, 045116 1–7.
- Samudrala, G. K., Tsoi, G. M., Weir, S. T., & Vohra, Y. K. (2014). Magnetic ordering temperatures in rare earth metal dysprosium under ultrahigh pressures. *High Pressure Research*, 34, 266–272.
<https://doi.org/10.1080/08957959.2014.903946>
- Samudrala, G. K., & Vohra, Y. K. (2013). Structural properties of lanthanides at ultra high pressure. In J.-C. G. Bünzli & V. K. Pecharsky (Eds.), *Handbook on the physics and chemistry of rare earths* (Vol. 43, pp. 275–319). Amsterdam: Elsevier.
- Thomas, S. A., Montgomery, J. M., Tsoi, G. M., Vohra, Y. K., Chesnut, G. N., Weir, S. T., ... dos Santos, A. M. (2013). Neutron diffraction and electrical transport studies on magnetic ordering in terbium at high pressures and low temperatures. *High Pressure Research*, 33, 555–562.
<https://doi.org/10.1080/08957959.2013.806503>
- Thomas, S. A., Tsoi, G. M., Wenger, L. E., & Vohra, Y. K. (2011). Magnetic and structural phase transitions in erbium at low temperatures and high pressures. *Physical Review*, B84, 144415 1–5.
- Toby, B. H. (2001). EXPGUI, a graphical user interface for GSAS. *Journal of Applied Crystallography*, 34, 210–213.
<https://doi.org/10.1107/S0021889801002242>
- Tsoi, G., Stemshorn, A. K., Vohra, Y. K., Wu, P. M., Hsu, F. C., Huang, Y. L., ... Weir, S. T. (2009). High pressure superconductivity in iron-based layered compounds studied using designer diamonds. *Journal of Physics: Condensed Matter*, 21, 232201 1–4.
- Wilkinson, M. K., Koehler, W. C., Wollan, E. O., & Cable, J. W. (1961). Neutron diffraction investigation of magnetic ordering in dysprosium. *Journal of Applied Physics*, 32, S48–S49.
<https://doi.org/10.1063/1.2000493>
- Yen, J., & Nicol, M. (1992). Temperature dependence of the ruby luminescence method for measuring high pressures. *Journal of Applied Physics*, 72, 5535–5538.
<https://doi.org/10.1063/1.351950>



© 2017 The Author(s). This open access article is distributed under a Creative Commons Attribution (CC-BY) 4.0 license.

You are free to:

Share — copy and redistribute the material in any medium or format

Adapt — remix, transform, and build upon the material for any purpose, even commercially.

The licensor cannot revoke these freedoms as long as you follow the license terms.

Under the following terms:

Attribution — You must give appropriate credit, provide a link to the license, and indicate if changes were made.

You may do so in any reasonable manner, but not in any way that suggests the licensor endorses you or your use.

No additional restrictions

You may not apply legal terms or technological measures that legally restrict others from doing anything the license permits.

